Kinetic Analysis of Folding and Unfolding the 56 Amino Acid IgG-Binding Domain of Streptococcal Protein G†

Patrick Alexander, John Orban, and Philip Bryan*

Center for Advanced Research in Biotechnology, Maryland Biotechnology Institute, 9600 Gudelsky Drive, Rockville, Maryland 20850

Received April 10, 1992; Revised Manuscript Received May 20, 1992

ABSTRACT: The 56 amino acid B domain of protein G (G_B) is a stable globular folding unit with no disulfide cross-links. The physical properties of G_B offer extraordinary flexibility for evaluating the energetics of the folding reaction. The protein is monomeric and very soluble in both folded and unfolded forms. The folding reaction has been previously examined by differential scanning calorimetry (Alexander et al., 1992) and found to exhibit two-state unfolding behavior over a wide pH range with an unfolding transition near 90 °C (G_{B1}) at neutral pH. Here, the kinetics of folding and unfolding two naturally occurring versions of G_B have been measured using stopped-flow mixing methods and analyzed according to transition-state theory. G_B contains no prolines, and the kinetics of folding and unfolding can be fit to a single, first-order rate constant over the temperature range of 5–35 °C. The major thermodynamic changes going from the unfolded state to the transition state are (1) a large decrease in heat capacity (ΔC_p), indicating that the transition state is compact and solvent inaccessible relative to the unfolded state; (2) a large loss of entropy; and (3) a small increase in enthalpy. The most surprising feature of the folding of G_B compared to that of previously studied proteins is that its folding approximates a rapid diffusion controlled process with little increase in enthalpy going from the unfolded to the transition state.

Protein G is a multidomain component of the cell wall of some streptococcal species and binds to all subclasses of human IgG by the constant Fc region. It is organized into functional domains similar to those of staphylococcal protein A (Åkerstrom & Björck, 1986), and the IgG-binding domains are similar in size. The IgG-binding function of protein G is contained in a globular domain of 56 amino acids designated G_B (Fahnestock et al., 1986). The basic folding pattern of the G_B domain consists of a four-stranded β-sheet spanned by an α-helix (Figure 1). No homology exists between the IgG-binding domains of protein A and protein G on the levels of either primary or tertiary structure. The isolated G_B domain is on the lower limit in size for a stable unique protein structure, yet it achieves its stability without disulfide bonds or tight ligand binding. In most general features, the thermodynamics of the folding reaction are similar to monomeric, globular proteins of much larger size (Alexander et al., 1992). Its small size permits the application of numerous biophysical techniques to study the folding and stability.

We have previously cloned and expressed two naturally occurring variations of the IgG-binding domain (G_{B1} and G_{B2}) of streptococcal protein G and characterized the thermodynamics of the unfolding reaction (Alexander et al., 1992). G_{B1} and G_{B2} differ by six amino acid substitutions (Figure 2) and have reversible two-state unfolding transitions over a wide range of pH. The structures of G_{B1} and G_{B2} have been studied by two-dimensional NMR[1] methods (Lian et al., 1991; Gronenborn et al., 1991; Orban et al., 1992). The physical properties of G_B offer extraordinary flexibility for evaluating the energetics of the folding reaction. The protein is monomeric and very soluble in both folded and unfolded forms. As will be described below, the folding reaction can be described in terms of a two-state reaction:

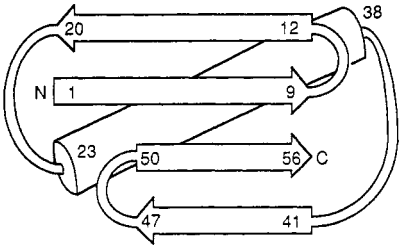

FIGURE 1: Schematic diagram of the global fold of G_B.

$$N \underset{k_f}{\overset{k_u}{\rightleftharpoons}} U$$

where k_u and k_f are first-order rate constants for unfolding and folding, respectively. The thermodynamics of the folding reaction over the pH range of 2.0–11.2 have been examined by DSC (Alexander et al., 1992). At pH 5.4, G_{B1} has a thermal denaturation temperature of 87.5 °C and G_{B2}, 79.4 °C. Here, we compare the kinetics of the unfolding and refolding reactions of G_{B1} and G_{B2} and characterize the thermodynamics of the transition state.

MATERIALS AND METHODS

Stopped-Flow Kinetic Measurements. G_B was purified as previously described (Alexander et al., 1992). The unfolding and refolding reactions were followed by monitoring the change in extinction at 293 or 250 nm on a Hi-Tech SF-51 stopped-flow spectrophotometer interfaced with a Compac 386 PC.

† This work was supported by NIH Grant 42560 and the Maryland Biotechnology Institute.

* Corresponding author.

[1] Abbreviations: CD circular dichroism; ΔH_{cal}, calorimetric enthalpy for unfolding; ΔH_{vH}, van't Hoff enthalpy for unfolding; ΔS_{ce}, chain entropy; ΔS_ϕ, entropy due to the hydrophobic effect; DSC, differential scanning calorimetry: EDTA, disodium salt of the ethylenediaminetetraacetic acid; N, native state; NMR, nuclear magnetic resonance; [P], protein concentration; PAGE, polyacrylamide gel electrophoresis; T, temperature; T_m, temperature of thermal melting; TS, transition state; U, unfolded state.

0006-2960/92/0431-7243$03.00/0

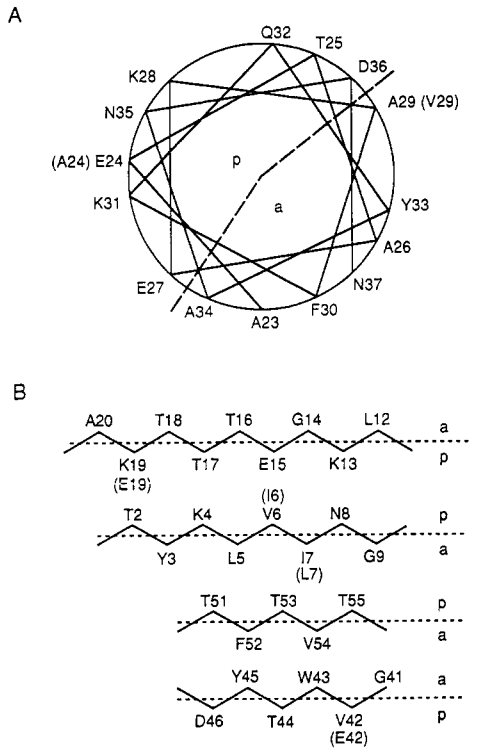

FIGURE 2: Secondary structure elements in G_B, illustrating the polar (p) and apolar (a) regions in the α-helix (A) and the β-sheets (B). The six amino acid substitutions found in G_{B1} are shown in parentheses.

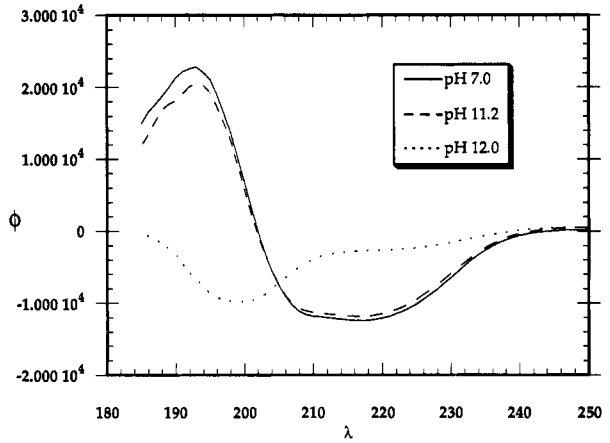

FIGURE 3: CD spectra of G_{B1}. Spectra were obtained in a Jasco 720 spectropolarimeter using a water-jacketed cell of 0.1-mm path length at 25 °C in potassium phosphate buffer at the indicated pH's.

Temperature was controlled by a circulating water bath with the two mixing syringes completely immersed in the thermostated water. A temperature probe embedded in a metal block surrounding the optical chamber indicated the temperature. A final mixing volume of 200 μL was achieved by injection of 100 μL from each syringe driven by a pneumatic piston. All solutions used in stopped-flow experiments were filtered by sterile 0.2-μm Acrodisc syringe filters (Gelman Sciences) to remove any particulates. The filters were thoroughly washed with 50 mL of the appropriate buffer to rinse away any organic contaminants present on the membranes.

To monitor the unfolding reaction, lyophilized G_B was rehydrated in deionized distilled water to a concentration of approximately 0.5 mg/mL and loaded in one of the syringes; 0.2 M potassium phosphate, pH 12.0, was added into the other. The solutions were mixed yielding 0.25 mg/mL G_B 0.1 M potassium phosphate, pH 12. G_B is completely denatured in 0.1 M phosphate, pH 12.0, at 25 °C (see below).

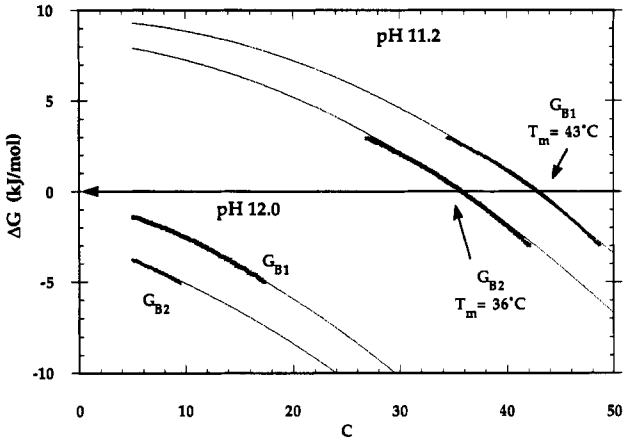

FIGURE 4: Stability profiles of G_{B1} and G_{B2} at pH 11.2 and 12.0. Heavy lines represent ΔG for unfolding computed from CD melting data. The thin lines are curves fitted to the equation $\Delta G = \Delta H_0 - T\Delta S_0 + \Delta C_p(T - T_0 - T \ln (T/T_0))$, where ΔH_0 and ΔS_0 are the enthalpy and entropy of unfolding evaluated at reference temperature T_0 (see text).

The refolding was achieved by a pH jump and was monitored by starting with denatured G_B ~0.5 mg/mL, 0.1 M potassium phosphate, pH 12.0, in one syringe and 0.1 M potassium phosphate, pH 7, in the other. Mixing in this instance yields 0.25 mg/mL G_B, 0.1 M potassium phosphate, pH 11.2. Time scales varied from 0.02 to 1 s at temperatures from 5 to 35 °C.

Circular Dichroism. All CD measurements were performed with a Jasco 720 spectropolarimeter using a 0.1-mm water-jacketed cell. Temperature control was provided by a Neslab RTE-110 circulating water bath interfaced with a MTP-6 temperature programmer. Protein solutions were 3 mg/mL in 0.1 M potassium phosphate buffers.

RESULTS

Thermodynamics of Unfolding

G_B maintains its native structure at 25 °C over the pH range of 1.5–11.0. The kinetic studies of folding reported here were carried out at pH 11.2. At neutral pH, the rate of folding is too rapid to measure by conventional stopped-flow methods, as will be described below in detail. In order to better interpret the kinetic results, the stability of G_{B1} and G_{B2} in the high pH range were examined by circular dichroism. At pH 12.0, both G_{B1} and G_{B2} are completely denatured at 25 °C. The CD spectra of the G_{B1} domain at pH 7.0, 11.2, and 12.0 are shown in Figure 3. At pH 11.2, the melting temperature of G_{B1} is 43 °C and of G_{B2} is 36 °C as determined by CD melting. These values are in good agreement with the T_m of G_{B1} determined at pH 11.2 by DSC (Alexander et al., 1992). The unfolding reaction at pH 11.2 was previously determined by DSC to follow a two-state model for unfolding, consistent with equilibrium thermodynamics as expressed in the van't Hoff equation, $(d \ln K)/dT = \Delta H_{vH}/(RT^2)$, with ΔH_{vH}, the van't Hoff enthalpy, or apparent enthalpy, equal to the calorimetric, ΔH_{cal}, or true enthalpy. From CD melting experiments at pH 11.2 and 12.0, the $\Delta G_{unfolding}$ was determined as a function of temperature (Figure 4). At pH 12.0, ΔG for both proteins is <0 at all temperatures with the maximum stability of the folded state occurring around 0 °C. The equilibrium constant for folding can only be determined in the CD at temperatures close to the T_m, where the fraction of both folded and unfolded forms can be accurately measured. The

Table I: Thermodynamic Parameters of the Folding Reaction[a]

	ΔG (kJ/mol)	ΔH (kJ/mol)	ΔS kJ/°mol	ΔC_p kJ/(deg·mol)
		pH 11.2, 25 °C		
G_{B1}				
U ⇒ TS	64.8	16.8	−0.161	−1.9
U ⇒ N	−6.1	−83.6	−0.260	−2.9
G_{B2}				
U ⇒ TS	62.4	15.3	−0.157	−2.0
U ⇒ N	−3.9	−93.9	−0.302	−2.9
		pH 12.0, 5 °C		
G_{B1}				
N ⇒ TS	69	109	0.144	0.9
N ⇒ U	−1.4	62	0.228	2.9
G_{B2}				
N ⇒ TS	65	102	0.134	0.9
N ⇒ U	−4.0	60.2	0.230	2.9

[a] Thermodynamic parameters for the U ⇒ TS and N ⇒ TS reactions were determined according to transition-state theory using the Eyring equation. Parameters for the U ⇒ N and N ⇒ U reactions were determined from CD melting experiments and eq 1 in the text. ΔC_p = 2.9 was previously determined by DSC (Alexander et al., 1992).

$\Delta G_{unfolding}$ can be extrapolated to temperatures beyond the experimentally observable range, however, using the Gibbs–Helmholtz equation:

$$\Delta G = \Delta H_0 - T\Delta S_0 + \Delta C_p(T - T_0 - T \ln (T/T_0)) \quad (1)$$

where ΔH_0 and ΔS_0 are the enthalpy and entropy of unfolding evaluated at a reference temperature T_0 and ΔG is the free energy of unfolding at temperature T (Brandts, 1964; Pace & Tanford, 1968; Privalov & Khechinashvili, 1974; Privalov, 1979; Becktel & Schellman, 1987). ΔC_p has been determined from calorimetric experiments to be 2.9 kJ/(deg·mol) (Alexander et al., 1992). The calculated curves shown in Figure 4 were generated by nonlinear least-squares fit of the data using eq 1 with ΔC_p = equal to 2.9 kJ/(deg·mol). Values of ΔG, ΔH, and ΔS obtained from the curve fitting are shown in Table I. The thermodynamic parameters obtained at pH 11.2 are in good agreement with the values obtained by DSC (Alexander et al., 1992). $\Delta G_{unfolding}$ at pH 11.2 and 25 °C is 6.1 and 3.9 kJ/mol for G_{B1} and G_{B2}, respectively. At pH 12.0 and 5 °C, $\Delta G_{unfolding}$ is −1.4 and −4.0 kJ/mol for G_{B1} and G_{B2}, respectively.

Dependence of T_m on pH. The melting transition temperature for G_B decreases rapidly above pH 11.0 due to the increasing negative charge of the protein. The change in the number of protons bound to the unfolded state (n_u) and the folded state (n_f) can be determined over the pH range 11–12 from the dependence of T_m on pH, according to the equation (Privalov, 1979)

$$n_u - n_f = (\Delta H/2.303RT_m^2)(\partial T_m/\partial \mathrm{pH}) \quad (2)$$

Sufficient data points were obtained over this pH range for G_{B1} to fit the T_m dependence on pH to the equation

$$T_m(\mathrm{K}) = 887 - 51(\mathrm{pH}) \quad (3)$$

Using ΔH = 84 kJ/mol, T_m = 298 K at pH 11.5, and the slope from eq 3, we calculate that 2.5 protons/molecule are released upon unfolding at pH 11.5. The T_m dependence of G_{B2} on pH is similar to that of G_{B1}. Presumably, this loss of protons upon unfolding at high pH is due to deprotonation of the three tyrosines in G_B as they are exposed to solvent. Two of the tyrosines (Y3 and Y45) are largely buried in the native protein, and the third (Y33) is partially buried (Gronenborn et al., 1991; Orban et al., 1992).

Table II: Rate Constants for Folding and Unfolding[a]

temp (°C)	folding rate constant (s^{-1}), pH 11.2		unfolding rate constant (s^{-1}), pH 12.0	
	G_{B1}	G_{B2}	G_{B1}	G_{B2}
5	7.9 ± 0.1	22.0 ± 0.3	0.71 ± 0.01	3.65 ± 0.05
10	12.5 ± 0.5	34.3 ± 1.2	1.28 ± 0.01	8.24 ± 0.1
15	16.9 ± 0.3	47.4 ± 0.9	3.03 ± 0.16	19.36 ± 0.3
20	21.3 ± 0.3	60.7 ± 2.1	7.21 ± 0.07	44.6 ± 0.6
25	25.5 ± 0.7	73.3 ± 2.7	17.1 ± 0.2	102 ± 1.0
30	32.9 ± 1.2	78.8 ± 4.7	43.2 ± 0.3	233 ± 7
35	29.9 ± 3.1		111.5 ± 1.5	447 ± 22

[a] Rate constants were determined by fitting spectroscopic data to a first-order kinetic equation. Values reported above are the average of five experiments for each condition.

Kinetics of Unfolding and Refolding

We have measured the rate of unfolding at pH 12.0 and the rate of refolding at pH 11.2. The unfolding and refolding rates are rapid and have been followed spectrophotometrically using a stopped-flow mixing device as described under Materials and Methods. In the refolding experiments the protein was denatured at pH 12.0 and then renatured by jumping the pH to 11.2. G_{B1} and G_{B2} contain one tryptophan and three tyrosines, which are largely buried in the native state. The extent of unfolding and refolding can be monitored by the change in tyrosine and tryptophan extinction vs time. The extinction coefficient at 293 nm decreases by 18% upon refolding at pH 11.2. At pH 12.0, E_{293} increases by 23% upon unfolding. The large changes in extinction upon unfolding and refolding at high pH presumably are due to the change in ionization of the three tyrosines as they are solvated during unfolding or desolvated during folding.

Refolding was monitored at high pH in order to slow the folding rate. At pH 6.6 and 25 °C, folding is complete in less than 2 ms (the mixing time of our stopped-flow cell). The first-order rate constants for refolding at 25 °C, pH 11.2, are 20.3 ± 0.3 s^{-1} for G_{B1} and 60.7 ± 2.1 s^{-1} for G_{B2} (Table II). The kinetic curves for both refolding at pH 11.2 and unfolding at pH 12.0 can best be fit to a first-order equation with a single rate constant. G_B contains no prolines which could introduce complexity in the refolding rate due to cis–trans isomerization. Examples of kinetic curves of G_{B1} refolding and the first-order fits are shown in Figure 5.

Temperature Dependence of the Refolding Rate. First-order rate constants (k) for folding at pH 11.2 over the temperature range of 5–35 °C are given in Table II. A plot of ln k vs $1/T$ is not linear, indicating that the folding reaction cannot be described in terms of simple Arrhenius theory. This behavior has been observed previously for the folding reaction of other proteins (Pohl, 1968; Chen et al., 1989; Jackson & Fersht, 1991). A change in heat capacity going from the unfolded state (U) to the transition state (TS) is expected since the overall $\Delta C_{p\ unfolding}$ is 2.9 kJ/mol and would explain the observed curvature in an Arrhenius plot.

To learn the general thermodynamic characteristics of the transition state, we have fit our data using transition-state theory according to the Eyring equation:

$$\Delta G^{\ddagger} = -RT \ln K^{\ddagger} = -RT \ln (kh/k_BT) \quad (4)$$

where k_B is the Boltzman constant, h is Planck's constant, and k is the first-order rate constant for folding. Graphs of ln (kh/k_BT) vs 1/T (in Kelvin) for folding are shown in Figure 6A. The data are fitted to the equation (Chen et al., 1989)

$$\ln K^{\ddagger} = A + B(T_0/T) + C \ln (T_0/T) \quad (5)$$

where $A = [-\Delta C_p^{\ddagger} + \Delta S^{\ddagger}(T_0)]/R$; $B = -A - \Delta G^{\ddagger}(T_0)/RT_0$;

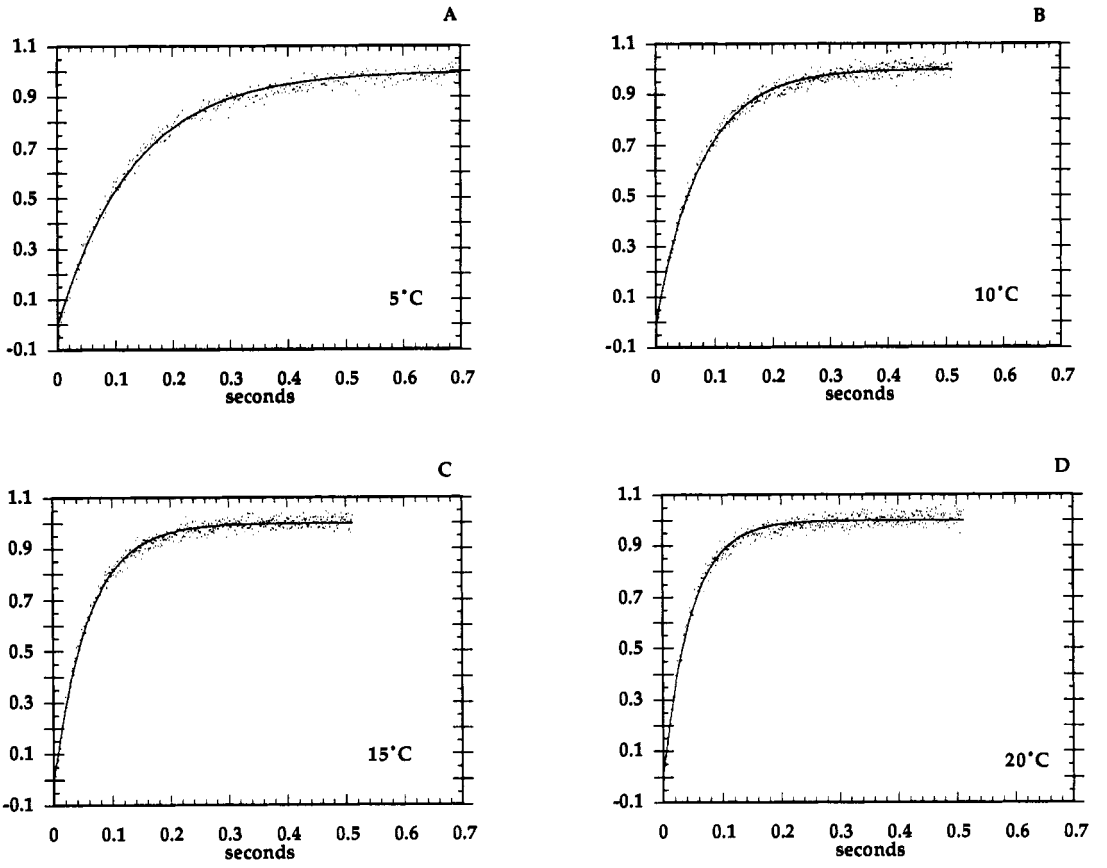

FIGURE 5: Kinetics of refolding G_{B1} as a function of temperature. Refolding kinetics were measured by stopped-flow absorption spectroscopy. Curves have been fitted to a first-order kinetic equation with a single rate constant.

$C = -\Delta C_p^{\ddagger}/R$. Thermodynamic parameters for the transition state for folding at pH 11.2 obtained from the fitted curves are summarized in Table I.

This treatment of the kinetic data is based on vibrational theory in which the frequency of breakdown of the transition state to product is equal to $\kappa k_B T/h$, where κ is a transmission coefficient assumed to be equal to one. As discussed previously by Chen et al. (1989, 1992), it is doubtful that this theoretical treatment is applicable to protein folding reactions in all respects; thus thermodynamic parameters determined for the transition state for the B domain should be viewed circumspectly.

The pronounced curvature of plots of the folding reaction is due to the large $\Delta C_p^{\ddagger}$ (–2 kJ/(deg·mol)). The change in heat capacity associated with formation of the transition state is about 70% of the total heat capacity change for folding ($\Delta C_{p\ \text{unfolding}}$ = 2.9 kJ/(deg·mol)). ΔC_p for protein folding has been shown to be closely correlated with the change in exposure of hydrophobic groups to water (Livingstone et al., 1991), thus the transition state (TS) appears to be compact and more similar to the fully native state (N) than to the unfolded state (U). Similar observations were made for a T4 lysozyme mutant in 3 M Gu-HCl (Chen et al., 1989) and for chymotrypsin inhibitor 2 (Jackson & Fersht, 1991). The values of $\Delta S^{\ddagger}$ indicate that entropy is lost going from the U to TS. There is also an overall loss in entropy going from the U to N at 25 °C. Because the folding reaction is a two-state process, we can calculate the rates of unfolding as a function of temperature at pH 11.2 according to the equation $\Delta G_{\text{unfolding}} = RT \ln (k_f/k_u)$. Calculated curves of $\ln K^{\ddagger}_u$ vs $1/K$ are also shown in Figure 6A. The intersection of the curves, where $k_f = k_u$, occurs at the T_m.

Temperature Dependence of the Unfolding Rate. First-order rate constants for unfolding at pH 12.0 over the temperature range of 5–35 °C are shown in Table II. A plot of $\ln k$ vs $1/T$ for the unfolding reaction is almost linear, indicating that the change in heat capacity going from the folded state to the transition state is small (Figure 6B). Thermodynamic parameters of the transition state for unfolding at pH 12.0, obtained from data fit to eq 5, are summarized in Table I.

Note that G_{B1} is thermodynamically more stable than G_{B2} at both pH 11.2 and 12.0 (Figure 6 and Table I). The rate of refolding, as well as unfolding, however, is slower for G_{B1} than G_{B2} (panels A and B in Figure 6). The same trends in stability and folding and unfolding rates for G_{B1} and G_{B2} are also observed at pH 11.6. The kinetic behavior indicates that TS of G_{B2} is more stable (lower energy) than TS of G_{B1}, unless there happen to be closely compensating changes in the energy of the folded and unfolded states of G_{B1} and G_{B2}.

DISCUSSION

Kinetic measurements are the only way to gain thermodynamic information about the transition state of folding, since it is too infrequently populated to be directly observed. Application of transition-state theory to kinetic data can yield specific thermodynamic information about the transition state for folding, subject to the accuracy of several assumptions which have been previously discussed in Chen et al. (1989, 1992). The major thermodynamic changes going from the unfolded state to the transition state are (1) a large decrease in heat capacity (ΔC_p), indicating that the transition state is compact and solvent inaccessible relative to the unfolded state; (2) a large loss of entropy; and (3) a small increase in enthalpy (Figure 7).

Entropic Changes in Folding. The $\Delta S_{\text{folding}}$ for G_{B1} was determined to be –0.26 kJ/(deg·mol) at pH 11.2 and 25 °C. This value results from the increased entropy from the loss

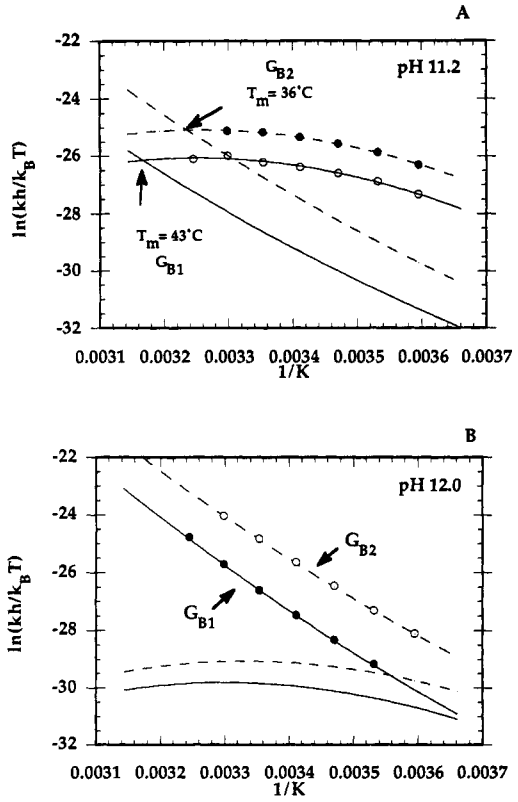

FIGURE 6: Temperature dependence of folding and unfolding rate of G_{B1} and G_{B2}. The natural log of the equilibrium constant for the transition state (ln (kh/k_BT)) is plotted vs the reciprocal of the absolute temperature. (A) Refolding data at pH 11.2 for G_{B1} and G_{B2} are fit according to eq 5 in the text with T_0 = 298 K. The corresponding curves for unfolding at pH 11.2 are calculated according a two-state unfolding model. The intersections of the folding and unfolding curves occur at the thermal denaturation temperatures for G_{B1} and G_{B2}. (B) Unfolding data at pH 12.0 for G_{B1} and G_{B2} are fit according to eq 5 in the text with T_0 = 298 K. The corresponding curves for refolding at pH 12.0 are calculated according a two-state unfolding model. The lack of points of intersection of the folding and unfolding curves indicates that $\Delta G_{unfolding} < 0$ at all temperatures for G_{B1} and G_{B2}.

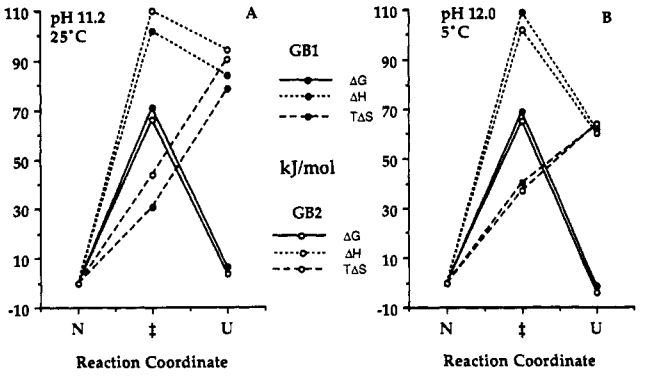

FIGURE 7: Reaction profile of folding process. Thermodynamic parameters ΔG, ΔH, and $T\Delta S$ are plotted vs the state of the protein as it proceeds from the U to TS to N at pH 11.2 and 25 °C (part A) and from N to TS to U at pH 12.0 and 5 °C (part B). The reference energies are arbitrarily set to the native state.

of ordered water due to the hydrophobic effect (ΔS_ϕ) being exceeded by the loss in entropy due to ordering the polypeptide (ΔS_{ce}). The ΔS_{ce} has been previously estimated to be ~ –0.9 kJ/(deg·mol) by extrapolating ΔS measurements made by DSC to 110 °C (Alexander et al., 1992). There is general agreement that the ΔS_ϕ vanishes near this temperature (Baldwin, 1986; Privalov & Gill, 1988). Thus, the residual ΔS at 110 °C can be attributed to chain entropy. The ΔS_{ce} value of ~ –16 kJ/(deg·mol) per residue for G_B is typical of other globular proteins. The extrapolation of ΔS measurements to 110 °C is probably reasonably accurate for G_{B1} since the melting temperature at pH 5.4 is 87.5 °C. At 87.5 °C, the experimentally determined $\Delta S_{folding}$ = –0.72 kJ/(deg·mol) (Alexander et al., 1992). Assuming that ΔS_{ce} is independent of temperature, then at 25 °C, ΔS_ϕ is equal to $\Delta S_{folding}$ (–0.26 kJ/(deg·mol)) – ΔS_{ce}(–0.9 kJ/(deg·mol)) = 0.64 kJ/(deg·mol).

The kinetic experiments described here show that $\Delta C_p^\ddagger$ = –2.0 kJ/(deg·mol), which indicates that ~70% of the native hydrophobic burial occurs in the transition state. One can calculate that most of the ordering of the polypeptide chain therefore must occur going from U to the TS as follows. There is a net loss of entropy going from U to TS at pH 11.2 and 25 °C ($\Delta S^\ddagger$ = –0.16 kJ/(deg·mol)). Thus, the gain in entropy from the hydrophobic effect is exceeded by the loss in entropy due to ordering the polypeptide with $\Delta S^\ddagger = \Delta S^\ddagger_\phi + \Delta S^\ddagger_{ce}$; 70% of ΔS_ϕ is 0.45 kJ/(deg·mol), so the predicted loss of chain entropy ($\Delta S^\ddagger_{ce}$) is –0.6 kJ/(deg·mol). Folding events going from TS to N result in the remaining 30% of the total hydrophobic burial, so remaining loss of chain entropy of going from TS to the native state is ~ –0.3 kJ/(deg·mol). In summary, about two-thirds of the chain entropy is lost going from U to TS, and the remaining one-third is lost going from TS to N.

Enthalpic Changes in Folding. The change in enthalpy going from U to TS is small compared to the enthalpic changes found for chymotrypsin inhibitor 2 (CI-2) (Jackson & Fersht, 1991) and an I3C–C97 disulfide mutant of T4 phage lysozyme (Chen et al., 1989). $\Delta H^\ddagger$ for T4 lysozyme is 22 kcal/mol (92 kJ/mol) at 12 °C at pH 5.0. $\Delta H^\ddagger$ for CI-2 is 12 kcal/mol (50 kJ/mol) at 25 °C and pH 6.3. By comparison, little enthalpic cost is required for G_B to go from the U to TS, with $\Delta H^\ddagger$ for G_{B1} = 16.8 kJ/mol at 25 °C and pH 11.2. We know that folding of G_B near pH 7.0 requires less than 2 ms. We can therefore put a lower limit on the rate constant for folding at pH 7.0 of ~10^3 s^{-1}. From our results at pH 11.2 and 12.0, $\Delta S^\ddagger$ appears to be relatively independent of pH (Figure 7). We therefore estimate that $\Delta H^\ddagger$ is ≤8 kJ/mol at pH 7.0. Thus, almost all the activation free energy for folding G_B at neutral pH is due to the loss of entropy going to the transition state. The folding of G_B therefore appears to be primarily a diffusion controlled process.

Structure of the Transition State. Presumably, as the protein condenses to the transition state, protein–protein interactions such as hydrogen bonds form in TS to compensate for the loss of protein–water hydrogen bonds in U. The specific protein–protein interactions that form in TS only roughly balance the loss of enthalpy from protein solvent interactions in U, however. A large decrease in enthalpy (–100 kJ/mol) drives the conversion of TS of G_{B1} to N at pH 11.2. One would assume that this large enthalpic change is due to the formation of many of the native protein–protein interactions such as hydrogen bonds. TS, though compact and solvent inaccessible relative to the unfolded form, would nevertheless appear to lack many of the native interactions.

The energy of TS is affected by six amino acid differences between G_{B1} and G_{B2} (I6V, L7I, E19K, A24E, V29A, E42V). G_{B1} is thermodynamically more stable than G_{B2} by about 2 kJ/mol at pH 11.2, but the TS of G_{B1} appears to be less stable (higher energy), resulting in both slower folding and unfolding. The slower folding and unfolding of G_{B1} could be due to its greater negative charge at alkaline pH. The increasing charge density as the protein becomes compact during early folding

may destabilize the TS of G_{B1} relative to G_{B2}. This seems to be reflected in the relative enthapies of the transition states. $\Delta H^{\ddagger}$ for G_{B1} is 1.5 kJ/mol greater than $\Delta H^{\ddagger}$ for G_{B2} (Table I). Once the native state is achieved, the charged residues are distributed such that the higher charge density of G_{B1} is no longer detrimental to stability.

The thermodynamic picture of the transition state for G_B is consistent with a compact form which nevertheless lacks many native protein–protein interactions. This state could be similar to the molten globule (A-state) in the model U ⇔ A ⇔ N (Kuwajima, 1989; Baldwin, 1989). Calorimetric studies have indicated that only small enthalpy changes accompany the transition from the A-state to the unfolded state [e.g., Bertazzon et al. (1990) and Xie et al. (1991)]. The A-state of most proteins is generally thought to be a low energy intermediate resulting from a rapid condensation of hydrophobic surface and occurring prior to the transition state [e.g., Garvey et al. (1989)]. For G_B, however, the A-state may be the highest energy state in the folding pathway. G_B does not appear to have a "high energy" transition state typical of larger proteins. The transition state of G_B seems to form in a diffusion controlled process and has only slightly higher enthalpy than the unfolded state. Perhaps, because of its small size, few enthalpically unfavorable structural adjustments may be required in going from the A-state to the native form of G_B. The hydrophobic core of G_B consists primarily of the conserved residues L5, A26, F30, W43, Y45, F52, and V54. In a protein with a larger hydrophobic core, the A-state may contain many more nonnative-like structures and require enthalpically unfavorable adjustments to reach the native state. Experiments are in progress using hydrogen–deuterium pulse-labeling and analysis by 2D-NMR methods, which should reveal more specific structural information about the folding pathway of G_B.

ACKNOWLEDGMENT

We thank John Moult for useful discussions about folding pathways and Matthew Mauro and Thomas Poulos for advice and assistance with stopped-flow spectroscopy.

REFERENCES

Åkerstrom, B., & Björck, L. (1986) *J. Biol. Chem. 261*, 10240–10247.

Alexander, P., Fahnestock, S., Lee, T., Orban, J., & Bryan, P. (1992) *Biochemistry 31*, 3597–3603.

Baldwin, R. L. (1986) *Proc. Natl. Acad. Sci. U.S.A. 83*, 8069–8072.

Baldwin, R. L. (1989) *Trends Biochem. Sci. (Pers. Ed.) 14*, 291–294.

Becktel, W. J., & Schellman, J. A. (1987) *Biopolymers 26*, 1859–1877.

Bertazzon, A., Tian, G. H., Lamblin, A., & Tsong, T. Y. (1990) *Biochemistry 29*, 291–298.

Brandts, J. F. (1964) *J. Am. Chem. Soc. 86*, 4291–4301.

Bryan, P. N., Rollence, M. L., Pantoliano, M. W., Wood, J., Finzel, B. C., Gilliland, G. L., Howard, A. J., & Poulos, T. L. (1986a) *Proteins: Struct., Funct., Genet. 1*, 326–334.

Chen, B., Baase, W. A., & Schellman, J. A. (1989) *Biochemistry 28*, 691–699.

Chen, B., Baase, W. A., Nicholson, H., & Schellman, J. A. (1992) *Biochemistry 31*, 1464–1476.

Dill, K. A., Alonso, D. O. V., & Hutchinson, K. (1989) *Biochemistry 28*, 5439–5449.

Fahnestock, S. R., Alexander, P., Nagle, J., & Filpula, D. (1986) *J. Bacteriol. 167*, 870–880.

Garvey, E. P., Swank, J., & Matthews, C. R. (1989) *Proteins: Struct., Funct., Genet. 6*, 259–266.

Gronenborn, A. M., Filpula, D. R., Essig, N. Z., Achari, A., Whitlow, M., Wingfield, P. T., & Clore, M. G. (1991) *Science 253*, 657–661.

Jackson, S. E., & Fersht, A. R. (1991) *Biochemistry 30*, 10436–19443.

Kuwajima, K. (1989) *Proteins: Struct., Funct., Genet. 6*, 87–103.

Lian, L. Y., Yang, J. C., Derrick, J. P., Sutcliffe, M. J., Roberts, G. C. K., Murphy, J. P., Goward, C. R., & Atkinson, T. (1991) *Biochemistry 30*, 5335–5340.

Livingstone, J. R., Spolar, R. S., & Record, M. T. (1991) *Biochemistry 30*, 4237–4244.

Orban, J., Alexander, P., & Bryan, P. (1992) *Biochemistry 31*, 3604–3611.

Pace, C. N., & Tanford, C. (1968) *Biochemistry 7*, 198–208.

Pantoliano, M. W., Whitlow, M., Wood, J. F., Dodd, S. W., Hardman, K. D., Rollence, M. L., & Bryan, P. N. (1989) *Biochemistry 28*, 7205–7213.

Pohl, F. M. (1968) *Eur. J. Biochem. 7*, 146–152.

Privalov, P. L. (1979) *Adv. Protein Chem. 33*, 167–241.

Privalov, P. L., & Khechinashvili, N. N. (1974) *J. Mol. Biol. 86*, 665–684.

Privalov, P. L., & Gill, S. J. (1988) *Adv. Protein Chem. 39*, 191–234.

Xie, D., Bhakuni, V., & Freire, E. (1991) *Biochemistry 30*, 10673–10678.